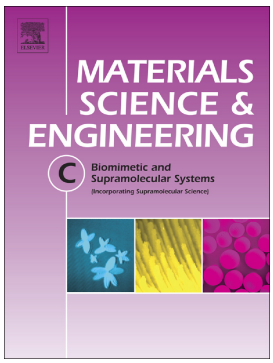

Fluorescence decay rate of selected compounds from Eysenhardtia polystachya extracts and their viability as biosensors

Ángel R. Hernandez-Martinez, Gustavo A. Molina, Angelina Rodríguez-Torres, Brenda Ledesma-Mendoza, Alicia Del Real, Joaquín Barroso-Flores, Miriam Estevez

PII: S0928-4931(19)31084-7
DOI: https://doi.org/10.1016/j.msec.2019.109978
Article Number: 109978
Reference: MSC 109978

To appear in: *Materials Science & Engineering C*

Received date: 1 April 2019
Revised date: 9 July 2019
Accepted date: 14 July 2019

Please cite this article as: Á.R. Hernandez-Martinez, G.A. Molina, A. Rodríguez-Torres, et al., Fluorescence decay rate of selected compounds from Eysenhardtia polystachya extracts and their viability as biosensors, Materials Science & Engineering C, https://doi.org/10.1016/j.msec.2019.109978

Fluorescence Decay Rate of Selected Compounds from *Eysenhardtia Polystachya* Extracts and their Viability as Biosensors

Ángel R. Hernandez-Martinez[1*], Gustavo A. Molina[2], Angelina Rodríguez-Torres[3], Brenda Ledesma-Mendoza[3], Alicia Del Real[1], Joaquín Barroso-Flores[4,5], & Miriam Estevez[1*]

[1]Centro de Física Aplicada y Tecnología Avanzada, Universidad Nacional Autónoma de México, Boulevard Juriquilla No. 3001, Querétaro, Querétaro, México, CP 76230.

[2]Posgrado en Ciencia e Ingeniería de Materiales, Centro de Física Aplicada y Tecnología Avanzada, Universidad Nacional Autónoma de México, Boulevard Juriquilla No. 3001, Querétaro, Querétaro, México, CP 76230.

[3]Universidad Autónoma de Querétaro, Unidad de Microbiología Básica y Aplicada. Camino a Chichimequillas, Ejido Bolaños, Querétaro, Querétaro, México. C. P. 76140.

[4]Centro Conjunto de Investigación en Química Sustentable UAEM-UNAM, Carretera Toluca-Atlacomulco Km 14.5, Personal de la UNAM, Toluca, Estado de México 50200, México.

[5]Instituto de Química, Universidad Nacional Autónoma de México, Ciudad Universitaria, Circuito Exterior s/n, Ciudad de México 04510, México.

*Author to whom correspondence should be addressed; e-mail: miries@fata.unam.mx; and angel.ramon.hernandez@gmail.com

Abstract

Eysenhardtia polystachya (EP) is an endemic Mexican plant that has been widely studied for its antidiabetic, antibacterial, and antioxidant properties. Several studies had reported the main components of EP, but their fluorescence properties had not been broadly studied. In a previous study we obtained extracts with different composition from this plant and they presented florescence. In this work we study fluorescent compounds from EP and evaluate their fluorescence properties. EP extracts were obtained by Soxhlet extraction with ethanol, samples were dried, and compounds were separated by column chromatography. Fluorescent fractions were classified apart from other fractions and characterized by Scanning electron microscopy (SEM), UV-vis, Raman, FTIR and ^{1}H NMR spectra. Additionally, we obtained functional nanomaterials (using silica nanoparticles). TD-DFT molecular calculations of the fluorescent components were carried out to compare their theoretical UV-Vis spectra to experimental results. Nine fractions were obtained by chromatography and five of them showed fluorescence. Fluorescence of extracts from *Eysenhardtia polystachya* is due to more than one component and we suggest that could be other hydrochalcones for which we present possible structures. This finding would help to dissipate questions about which component is responsible for fluorescence in extracts from the plant and in this way determinate the

appropriate use for these fluorophores. Finally, the application and viability as a biosensor using pulmonary epithelium fibroblast cell culture IMR-90 was proved, and in the concentration used are non-toxic materials.

Keywords: *Eysenhardtia polystachya*, fluorescence, functional material, biosensor, IMR-90 fibroblast

1. Introduction

Eysenhardtia polystachya (Ortega) Sarg. (Leguminosae:Lotoideae) is a tree distributed in Mexico and Texas, locally known as "*palo dulce*" (sweet wood), "*palo azul*" (blue wood), and kidneywood. It has been traditionally used for treating urinary tract and bladder infections, and as a diuretic by several Mexican indigenous groups within the large Mexican herbal tradition [1]. Between the sixteenth and seventeenth centuries it was known as *Lignum nephriticum* (kidneywood) in Europe [2]. Scientific reports have mentioned this tree since 1664 due to the blue fluorescence of its infusion in water [3]. It also has been studied because of its antidiabetic, antibacterial, and antioxidant properties [4].

Some efforts focused on plant composition, for example, Dominguez isolated 3,4-dimethoxy-8,9-(methylenedioxy)pterocarpan and dehydrorotenone[5]. Beltrami, et. al. isolated and elucidated two C-glicosil-α-hydroxydihydrochalcones which have diuretic properties [6]. Alvarez, et. al. isolated and elucidated two isoflavonoids and four α-hydroxydihydrochalcones, (3S)-7-hydroxy-2′,3′,4′,5′,8-pentamethoxyisoflavan, (3S)-3′,7-dihydroxy-2′,4′,5′,8-tetramethoxyisoflavan, (αR)-α,3,4,2′,4′-pentahydroxydihydrochalcone, (αR)-3′-C-β-d-xylopyranosyl-α,3,4,2′,4′-pentahydroxydihydrochalcone, (αR)-3′-O-β-d-xylopyranosyl-α,3,4,2′,4′-pentahydroxydihydrochalcone, and coatline B [(α R)-3′-C-β-d-glucopyranosyl-α,2′,3,4′,4-pentahydroxydihydrochalcone]. Alvarez results also showed that none of those molecules are toxic, which is important if they are used in medicine [1, 7]. In none the aforementioned studies fluorescence properties of the chemical species were reported.

Burns, et.al. reported in 1984 that 7-hydroxy-2',4',5'-trihydroxyisoflavone is one of the fluorescent phenolic constituents of a methanolic *Eysenhardtia polystachya* (*EP*) extract; that has strong blue fluorescence at λ =480 nm at pH 8.04 [8]. To our knowledge, Acuña, et. al. first reported fluorescent properties of *EP* components and they attributed fluorescence to a molecule formed by a spontaneous oxidation of a flavonoid (at least one). They reported that the four-ring tetrahydromethanobenzofuro[2,3-d]oxacine (matlaline) gives the intense blue fluorescence in a *EP* infusion. Acuña found that coatline A and B (molecules isolated from *EP*) oxidate at room temperature in the presence of slightly alkaline water solution (pH ~7.5); this reaction is fast, irreversible and a strongly blue-emitting compound is obtained. This compound was identified as matlaline with *c.a.* 100% yield and an intense fluorescence (λ=465 nm) that depends on pH of the solution [9].

On the other hand, the development of highly sensitive and selective methods for the detection of diverse pathologies can be strongly driven by intelligent man- made systems —based on artificial materials inspired in nature— [10-12]; or through of the setting-up of artificial active systems with kinetically

controlled dynamics inspired on living biological systems [13]. Novel techniques also could be developed from biosensor that uses intelligent materials and programming of chemical networks [14, 15]. In that sense, our group focused on possible uses of the extract in medicine. These previous studies allowed us to obtain a biomarker, in the form of a functionalized nanomaterial from silica and *Eysenhardtia polystachya* extracts, that was used to label MCF-7 tumor cells (ATCC) [4]. Then, we evaluated different extraction solvents and their effect on fluorescence of materials proposed as biomarkers; our results showed that extracts had different chemical species depending on solvents and some samples presented fluorescence [16]. Thus, the purpose of this work is to study different compounds of an ethanolic extract of *Eysenhardtia polystachya* obtained by column chromatography and evaluate their fluorescence properties in order to select the best compound and study its viability as a biosensor using pulmonary epithelium fibroblast cell culture as a model.

2. Materials and methods

2.1 Materials

Samples of *Eysenhardtia polystachya* heartwood from Uruapan, Michoacán which were previously identified as MEXU 1850 (National Herbarium, UNAM) were used through all the experiments reported hereby. Tetraethylorthosilicate (TEOS) (98%), 3-aminopropyltriethoxysilane (APTES), methanol (CH_3OH, MeOH), ethanol (C_2H_5OH, EtOH) (90%), toluene (C_7H_8), hexane ($CH_3(CH_2)_4CH_3$), ethyl acetate ($CH_3COOC_2H_5$, EtOAc) and silica gel (high-purity grade, pore size 60Å, 200-400 mesh particle size) were purchased from Sigma Aldrich Co. Ammonium hydroxide (NH_4OH), phthalate buffer solution (pH 4.0), monobasic sodium phosphate (NaH_2PO_4) and dibasic sodium phosphate (Na_2HPO4) were purchased from J.T. Baker. Phosphate buffer solution of pH 7.4 and pH 8 were prepared using adequate quantities of mono and dibasic sodium phosphate. All chemicals were used without further treatment and deionized water was used in all experiments.

2.2 *EP* compounds extraction, column and thin film layer chromatography

A piece of *EP* heartwood was slided, crushed into smaller pieces and grinded into a fine powder which was then subjected to an ethanolic Soxhlet extraction for 96 hours using a procedure previously reported[4, 16]. Solvent excess was evaporated at 40 ºC using reduced pressure (172 mbar) with a rotatory evaporator BÜCHI R-210 (BÜCHI, Switzerland) and samples were finally dried at 60 ºC for 12 hours to obtain the *EP* organic compounds (EPC). Samples were stored in amber glass vials, sealed, labeled and kept under controlled temperature for further use.

EPC were applied to Sigma Aldrich thin-layer chromatography (TLC) plates with standardized micropipettes. Those plates were placed inside a chromatography chamber with solvents of different polarities (from hexane to MeOH) to approximate the polarity of the substrates. A preliminary test of fluorescence of the compounds was performed in the chromatography chamber with the coupled ultraviolet light lamp (365 nm). Using these preliminary test, results indicate that the column chromatography should start with a mobile phase of hexane:EtOAc (1:1 v/v).

1 g of EPC and 4 g of silica gel were mixed, and 2 mL of EtOH were added to this mixture (sample FP-A). The lower part of the chromatography column was packed with cotton and 17.5 g of clean silica, and sample FP-A was placed into the column (weight ratio of 7:2 clean silica/FP-A). The top of the column was sealed with cotton. Chromatography column packing was eluted with hexane:EtOAc (1:1 v/v), followed by EtOAc (100%), ethyl EtOAc:EtOH (25:75 v/v) and quenched with MeOH (100%). By using the describe procedure, 71 fractions, each of approximately 40 mL, were collected. Fractions were immediately placed inside the rotatory evaporator (40 °C @ 230 mbar), one by one to remove the maximum amount of solvent. Later, fractions were grouped depending on their corresponding TLC plate. Nine groups of powder samples were classified, stored in amber glass vials, sealed, labeled and kept under controlled temperature for further use.

2.3 Spectroscopy techniques

Samples were characterized by spectroscopic techniques, such as UV-Vis spectrophotometry, which is a simple, fast, and highly reproducible technique for the detection of flavonoids [17-21]. UV-Vis spectra were recorded on a VWR 1600 PC spectrophotometer (NASDAQ: VWR, Radnor, Pennsylvania, USA) from 200 to 900 nm. The nine groups obtained were diluted in three buffer solutions; alkaline (pH 8.0), physiological (pH 7.4), acidic (pH 4.0) and they were placed in a quartz cuvette for analysis.

Raman spectra at room temperature were obtained to record the fluorescence signal by a micro Raman spectrometer LabRAM II (DILOR, Lille, France) equipped with a confocal optical microscope using silicon peak at 520 cm^{-1} as frequency standard. Ar-ion laser was used as excitation source at 480 nm (@ 30 mW) and data were collected in the range from 400 to 1000 nm. Approximately 0.01 g of the selected group sample were diluted in three different pH solutions; alkaline, acidic and physiological pH. Later, 5 mL of each solution were placed immediately in a quartz cuvette and fluorescence was evaluated every 45 s during the first 7 min; then every 5 min for 15 more minutes.

Proton nuclear magnetic resonance (^{1}H NMR) spectra of a selected sample was acquired on a Bruker Avance III HD 400 spectrometer, using deuteride DMSO as solvent and tetramethylsilane (TMS) as standard at 25 ºC. The chemical shift data is reported in parts per million (ppm) on the δ scale.

2.4 Synthesis of silica nanoparticles and preparation of functional materials

Silica nanoparticles (SiNp) were prepared according to a modified Stöber process for obtaining spherical monodisperse particles reported by Greasley [22]. The molar ratio between elements was 1:40:20:1 for TEOS, EtOH, deionized water and NH_4OH. EtOH, deionized water and TEOS were mixed in an ultrasonic bath during 10 min at room temperature. After elapsed time, NH_4OH was added dropwise to the solution and left in the ultrasonic bath for two more hours at 60 ºC. The final solution was left overnight to ensure particle maximum size. Then, solution was washed through centrifugation to obtain a particle pellet

which was dried once again overnight at 60 ºC. Finally, dried samples were pulverized in an agate mortar and placed in glass vials and stored in a humidity-free desiccator until further use.

Fluorescent fractions with the highest and lowest fluorescence extinction coefficient were selected, to obtain a functionalized nanomaterial using SiNp. Echeverrie, et.al. procedure was used with this purpose [23]. 1 g of monodispersed SiNp was diluted using toluene in a ball flask and 1 mL of APTES was added; the solution was kept under continuous stirring at 120 °C for 24 h using a reflux system. Then, solution was dried at 80 °C for 24 h, powdered and washed with EtOH and deionized water.0.2 g of powder was dispersed in deionized water with 1g of each selected fraction. The dispersion was kept under continuous agitation (500 rpm) at room temperature for 24 h and subsequently dried at room temperature. The powder obtained was pulverized in an agate mortar, placed in amber glass vials and stored in free humidity desiccator for further use. The morphology, size and shape of the SiNp and the functional materials were analyzed using scanning electron microscopy (SEM). SEM images were acquired with a high-resolution SEM microscope HITACHI SU8230 at 3.0 keV of acceleration voltage. A drop of the solution was deposited directly on Al stubs with carbon film for the observation.

2.5 Quantum mechanical calculations of fluorescent molecules

Density Functional Theory (DFT) based calculations at the M062X/6-311G(*d,p*) level of theory were taken to calculate the UV-Vis spectra for compounds G3,G5and G6 on their previously optimized geometries. All calculations were performed with the Gaussian 09 suite of programs [24]

2.6 Viability of selected organic compounds and functional materials as biosensors

2.6.1 Cell culture and treatment

Cells derived from immortalized nonpathological pulmonary epithelium IMR-90 fibroblast (ATCC CCL-186), were grown in DMEM medium, supplemented with 10% fetal bovine serum (FBS) and 1% antibiotic/antifungal. Cells were kept in incubation at 37 °C in a 5% CO_2 atmosphere. Cells were directly seeded in well for cell viability essay in to 18mm glass plates for confocal microscopy in a 12-well dish and treated at 70% confluency.

The treatment was performed under two conditions: **1)** cells treated with the selected compounds group (see results section 3.1, group G2) and **2)** cells treated with the functionalized SiNp compounds group (see results section 3.2, group N-G2). Solutions (originally in an ethanol matrix from the synthesis of nanoparticles or the components extraction) were diluted in DMEM supplemented with 1% FBS and 1% antibiotic/antifungal to the concentration of 100 µg/mL. DMEM added with proportional ethanol was used as a control. Cells were incubated with these solutions at 37 °C in a 5% CO_2 atmosphere for 24 h.

2.6.2 Confocal laser microscopy

After treatment, cells were washed twice with phosphate buffer saline (PBS 1X pH 7.4) and then fixed for 30 min with 3.7% paraformaldehyde in PBS, at room temperature. For the nucleus labeling, cells were incubated with DAPI 1µg/mL for 15 min and then washed three times, with PBS 1X, distilled water and double-distilled water respectively. Next, glass plates were mounted on slides for the observation in confocal microscope. Cells were visualized using a confocal microscope LSM 880 (Carl Zeiss, Oberkochen, Germany) in bright field and at the wavelengths of 405 nm for DAPI labeling and 488 nm for G2 fluorescence labeling.

2.6.3 Cellular viability assay

Cellular viability was calculated by a trypan blue exclusion test. Cells were centrifuged for 5 min at 4500 g, the supernatant was discarded, and the cell pellet was resuspended in 1 mL of DMEM medium. Then, 10 µL of the cell suspension was mixed with trypan blue 0.4% in a 1:1 ratio and 10 µL of this mix was applied into a hemocytometer. Viable (unstained) and non-viable (stained) cells were counted by placing the hemacytometer on the stage of an optical Axiovent 25 microscope (Carl Zeiss, Oberkochen, Germany). The percentage of viability was calculated through equation 1:

$$\text{Viability } \% = \frac{\text{Total number of viable cells per mL}}{\text{Total number of cells per mL}} \text{ x } 100 \quad \text{..... (Eq. 1)}$$

3. Results and discussion

3.1 Organic compounds characterization

As mentioned in the methods section, a preliminary test of fluorescence allowed obtaining the appropriate solvent for eluting compounds, which had a 0.5 retention factor. Results indicated that an appropriate solvent mixture was (hexane:EtOAc; 1:1 v/v). The fractions obtained were classified into 9 groups (G1 to G9) considering similar chromatographic profile (verified by TLC) and UV-Vis spectra. Five of these groups presented fluorescence (Table 1).

Table 1. Ethanolic fractions of *Eysenhardtia polystachya* by column chromatography

Organic compound (Group)	Fractions grouped	Fluorescence (365 nm)
G1	F1 to F8	No
G2	F9 to F16	Yes
G3	F17 to F20	Yes
G4	F21 to F24	Yes
G5	F25 to F35	Yes
G6	F36 to F48	Yes
G7	F49 to F53	No

G8	F54 to F60	No
G9	F60 to F71	No

UV-Vis spectra of the fluorescent groups were obtained (Figure 1). Maximum absorptions of these five groups (G2 to G6) were at c.a. 290 and 325 nm, these peaks alone could indicate the presence of chalcones or/and flavonoids skeleton, such as mentioned in a previous study in which the UV-Vis spectrum of fraction G3 was also found for an ethanolic extract from *Eysenhardtia polystachya (Ortega) Sarg*[4]. In that report, the peaks of the spectrum were attributed to a mixture of chalcones and flavonoids based on colorimetric results obtained in a Shinoda test and in Alvarez results [7] on isoflavonoids.

As mentioned before, In the current study, it was isolated five fluorescent groups, which are in agreement to data reported by Alvarez [7] for their four-hydroxydihydrochalcones and by Acuña[9] for coatline A that reported maximum absorptions c.a. 285 and 322 nm. A schematic representation of these five α-hydroxydihydrochalcones is shown at the end of Figure 1.

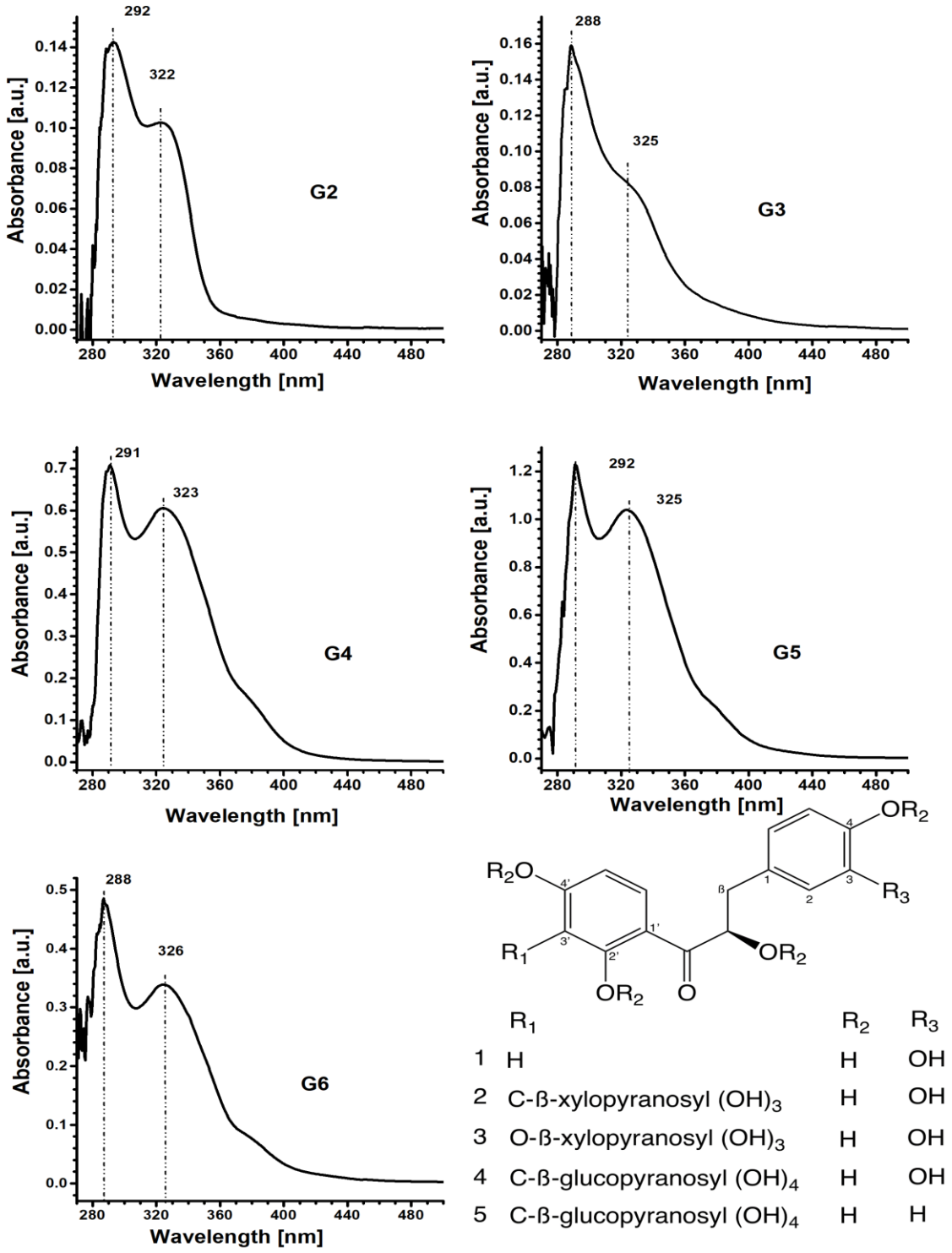

Figure 1. UV–Vis spectra of organic compounds from *Eysenhardtia polystachya* with photoluminescence (groups G2 to G6) at pH 7.4, and schematic representation of these compounds (α-hydroxydihydrochalcones); where the numerals from 1 to 5 indicate the substitutes "R" corresponding to each α-hydroxydihydrochalcones.

To elucidate the chemical species in fluorescent fractions, we supposed that hydrochalcones present in the ethanolic extract of EP could have a spontaneous oxidation at room temperature and products could be oxacines (Figure 2). These suggestions are supported on Acuña's assumption that the blue fluorescence of EP infusion is due to a novel four-ring tetrahydromethanobenzofuro[2,3-d]oxacine (matlaline) which is not present in the plant but is the end product of an spontaneous oxidation from coatline A and B (both water-soluble α-hydroxydihydrochalcones) at room temperature and in slightly alkaline (pH ~7.5) water solution, as mentioned in the introduction [9].

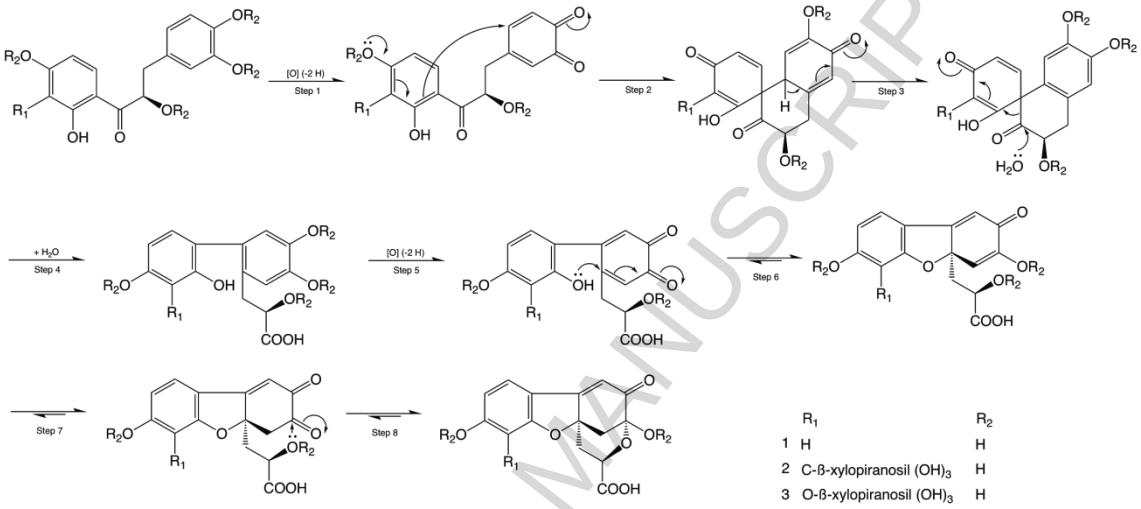

Figure 2. Schematic sequential reaction from α-hydroxydihydrochalcones into tetrahydromethanobenzofuro[2,3-d]oxacine at room temperature in water solution based on report of Acuña [9]

The differences between maximum wavelength of UV–Vis absorption and maximum emission at the same electronic transition (Stokes shift) are shown in Figure 3. Energy difference between absorption and emission spectra and probability of electronic transition or molar extinction coefficient (Log ε) data for the five groups or chemical compounds that presented luminescence are shown in Table 2. These Log ε values correspond to data obtained by Alvarez [25] for α-hydroxydihydrochalcones.

Typical Jablonski diagram (Figure 3) illustrates the singlet ground (S_0) state, as well as the first (S_1) and second (S_2) excited singlet states as a package of horizontal lines, which clearly exemplifies excitation or absorption and emission from fluorescent processes of the hydroxydihydrochalcones/oxacines.

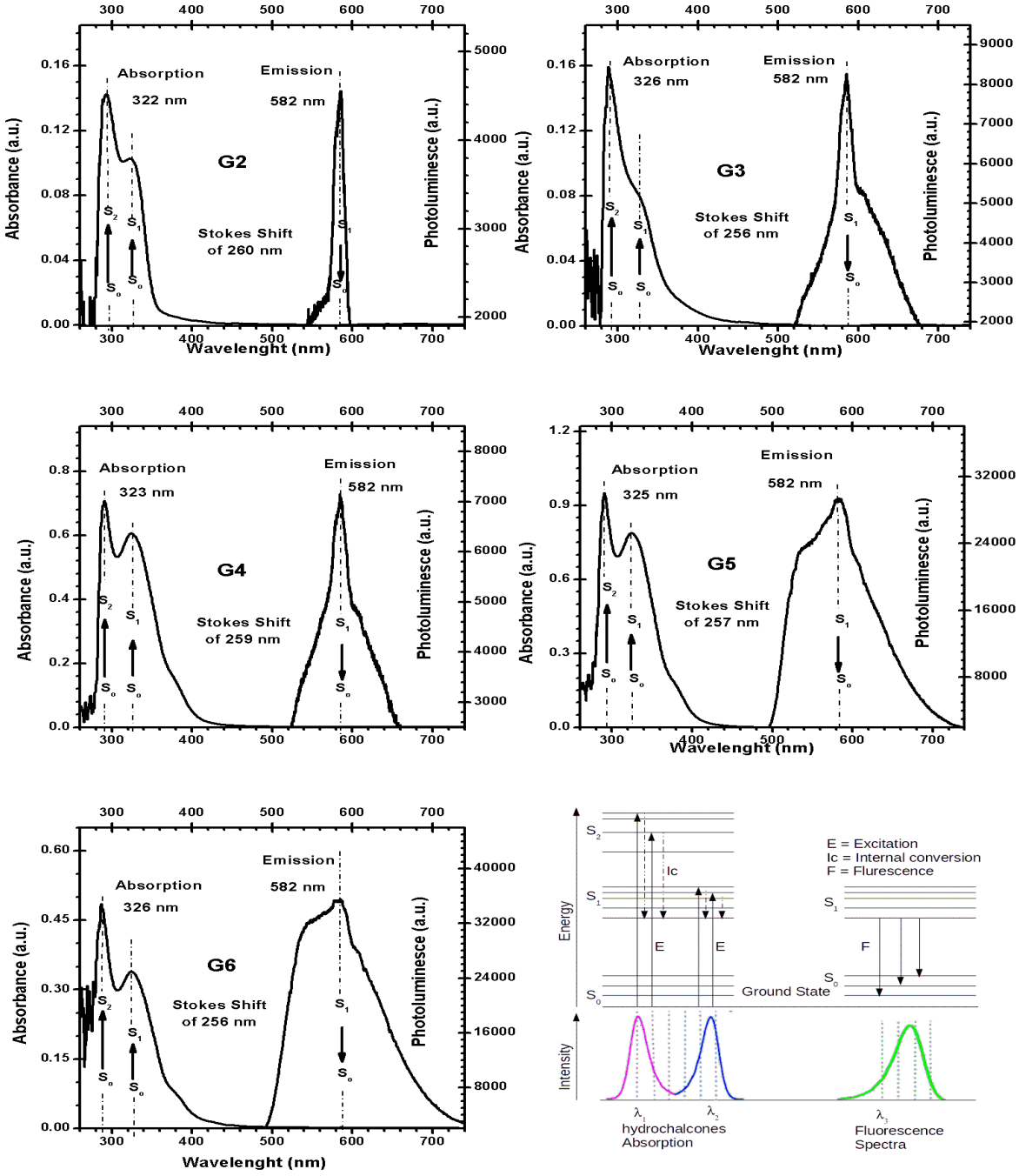

Figure 3. UV–Vis and fluorescence spectra of groups G2 to G6 showing Stokes shift at pH 7.4

Fluorescence was influenced by pH as seen in Table 2. G2 and G4 did not present fluorescence at acidic pH due to secondary chemical species produced during a reaction induced by pH of the medium. Fractions fluorescence at pH 7.4 (considered as a physiological condition) is an interesting finding, because it means that these compounds from EP have a high potential for usage in biological models for application.

Table 2. Chemical species photoluminescence, Stokes Shift (nm) and extinction coefficient

Molecule set	Log ε (pH 7.4, λ=322)	Log ε (pH 7.4, λ=290)	Stokes Shift (nm) pH 8.0	Stokes Shift (nm) pH 7.4	Stokes Shift (nm) pH 4.0
G2	2.89	3.12	258	277	0*
G3	3.20	3.16	280	265	175
G4	2.84	3.08	274	267	0*
G5	2.88	3.31	271	259	175
G6	3.22	3.17	207	207	112

* No luminescence was presented

UV absorption bands of G6 could correspond to aurones, specifically matlaline based on published reports [10, 26, 27]. Chemical species of G2; G3; G4; and G5 also presented luminescence and could correspond to flavanonols and flavanones comparing our results with Acuña et al. report[8-16].

3.2 Fluorescence spectra analysis of organic compounds

The Raman spectra to study the luminescence of every group were recorded with a total radiation exposure time of 65 min. Sample evaporation was avoided by controlling temperature at 25 ºC and keeping quartz cuvette closed during the experiments. Hence, decrease in fluorescence intensity could only be attributed to a structural change in chromophore molecules responsible of fluorescence.

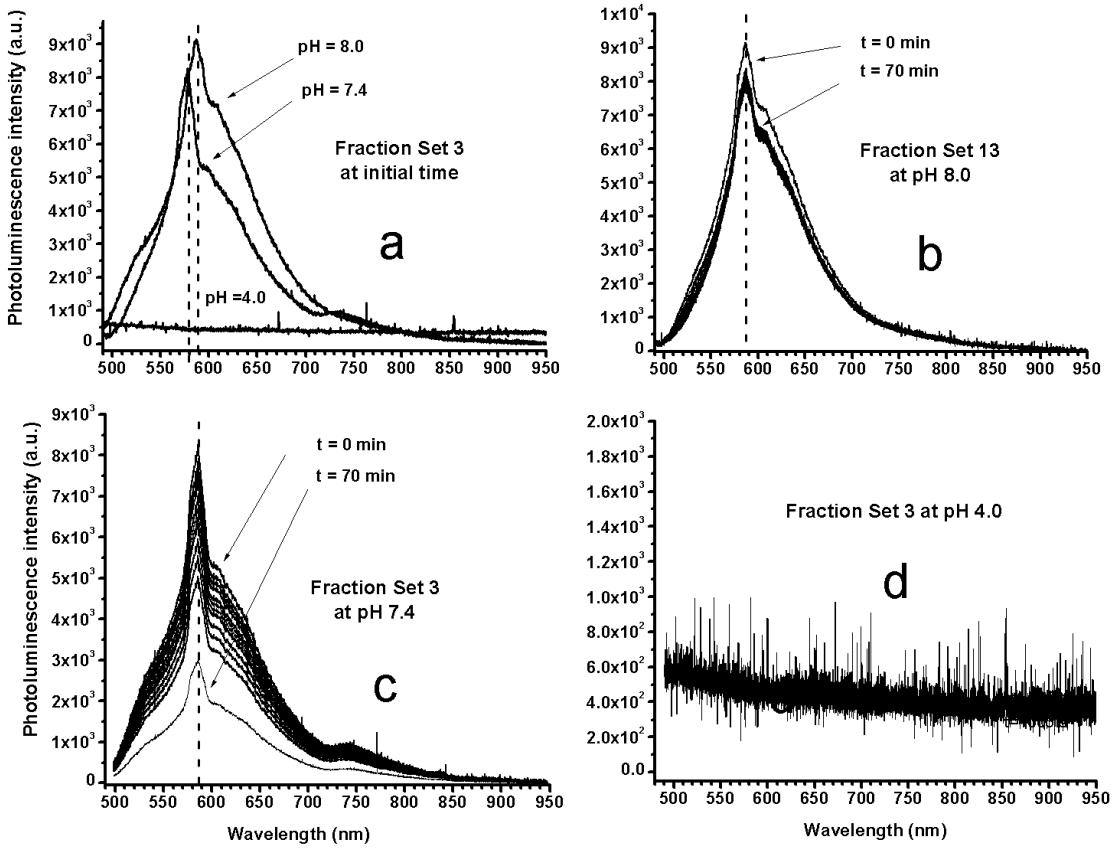

Figure 4. Example of obtained Raman spectra on fluorescence behavior (group G3) as a function of: a) pH, b) time at pH 8, c) time at pH 7.4 and d) time at pH 4.0.

Figure 4 shows G3 photostability as a function of both the pH medium and time. Fluorescence was favored at alkaline pH (Figure 4.a) since about 9,000 photons were counted, while 8,000 and 500 photons were detected at physiological pH and acidic pH respectively; i.e., counts decreased in 84.5% changing only the initial alkaline pH to acid pH of the sample at t=0. Then, fluorescence is greater in basic medium than in acid medium. These data are coherent compared with the reported behavior that is attributed to ionizing effect of the medium [16, 28].Figure 4.b, c and d show fluorescence reduction over time at different pH conditions.

To summarize, fluorescence intensity decays over time and it is directly dependent on pH medium. Fluorescence intensity as function of time was analyzed deeply; and using the criteria described previously [10] to study permanent fluorescence loss. In Figure 5 are the fluorescence intensity (*PLi*) for the six fractions at alkaline and physiological pH. The fluorescence at acid pH was not shown because in all cases it presented the same characteristics shown in Figure 4d and can't be analyzed.

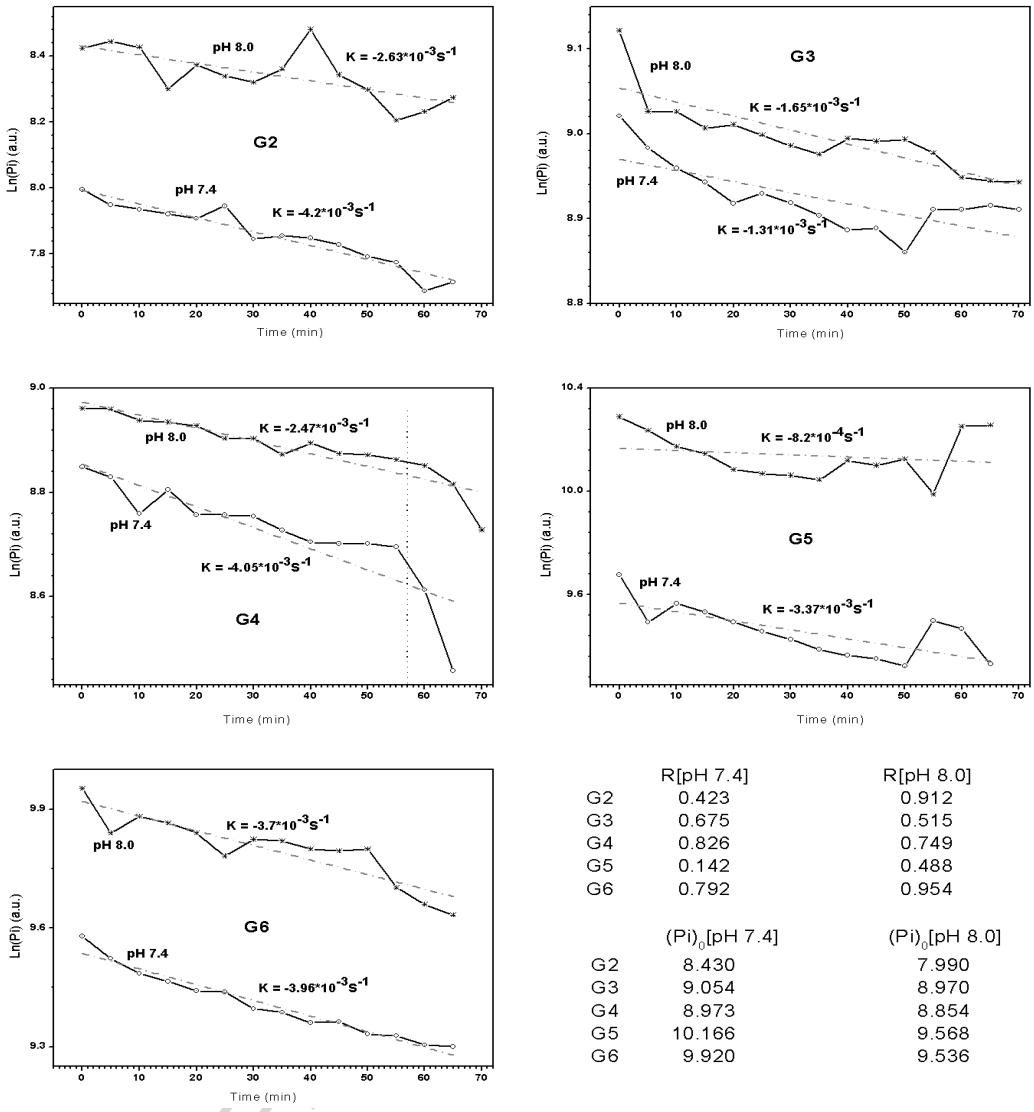

	R[pH 7.4]	R[pH 8.0]
G2	0.423	0.912
G3	0.675	0.515
G4	0.826	0.749
G5	0.142	0.488
G6	0.792	0.954

	$(Pi)_0$[pH 7.4]	$(Pi)_0$[pH 8.0]
G2	8.430	7.990
G3	9.054	8.970
G4	8.973	8.854
G5	10.166	9.568
G6	9.920	9.536

Figure 5. Fluorescence Intensity plots at physiological an alkaline pH media for groups G2 to G6

PLi data were adjusted and its loss behavior was described by a first order exponential decay model as a function of the irradiation time, as follows:

$$PLi = (PLi)_0 \cdot e^{-(kt)}$$

where *PLi* represents the fluorescence intensity at a given time *t*; $(PLi)_0$ is the initial fluorescence intensity at time *t*=0 and *k* is the constant decay rate of the fluorescence intensity in min^{-1}. By plotting the ln(*PLi)* behavior, the model proposed could be written as a linearization:

$$\ln(PLi) = \ln(PLi)_0 - kt$$

Observing the proportion of variance in *PLi* on the linear regression —R squared— in Figure 5, it can be seen that the exponential decay model fits consistently to the experimental data and the constant rate *k*

describes the fluorescence extinction constant. G2 and G4 were the most and the least stable set of molecules with a 7.81% (at pH 7.4) and 32.38% (at pH 8.0) *PLi* losses, respectively (Table 3).

Table 3. Constants rates and percentage of fluorescence intensity (*PLi*) decay

Molecule set	pH	R^2	k [m^{-1}]	*PLi* decay [%]
G2	7.4	0.912	$-4.20*10^{-3}$	7.81
	8.0	0.422	$-2.63*10^{-3}$	24.40
G3	7.4	0.510	$-1.31*10^{-3}$	10.43
	8.0	0.693	$-1.65*10^{-3}$	16.37
G4	7.4	0.739	$-4.05*10^{-3}$	20.82
	8.0	0.826	$-2.47*10^{-4}$	32.38
G5	7.4	0.489	$-3.37*10^{-3}$	25.94
	8.0	0.244	$-8.20*10^{-3}$	29.36
G6	7.4	0.954	$-3.96*10^{-3}$	27.37
	8.0	0.792	$-3.70*10^{-3}$	24.40

G2 was the most stable set of molecules at physiological pH with a 7.81% *PLi* decay, k value of -4.20E10^{-3} and R-square of 0.912. On the other hand, G3 was the most stable set of molecules at alkaline pH with 16.37% *PLi* decay, k value of -1.65E10^{-3} and R-square of 0.693. G6 and G4 were the least stable molecules at physiological and alkaline pH, respectively.

After comparing decay of fluorescence intensity as a function of time in each set fluorescent molecules, it was decided to synthesize two functional materials, the first one using G2 (the lowest decay at pH 7.4) and the second using G6 (the highest decay at pH 7.4).

As seen in Figure 6 it can be seen the SEM images for the SiNp and the functional materials.It is showed in Figure 6.a, that SiNp used for the functional material has an average size of 94nm with a semi-regular spherical shape and on the other hand in Figure 6.b it can be seen that the functional material has a slightly different morphology since it is not completely spherical since there is agglomeration and also it can be seen a change in contrast on the surface indicating that the organic compound are there and it can be seen an increase on the average size of 146 nm.

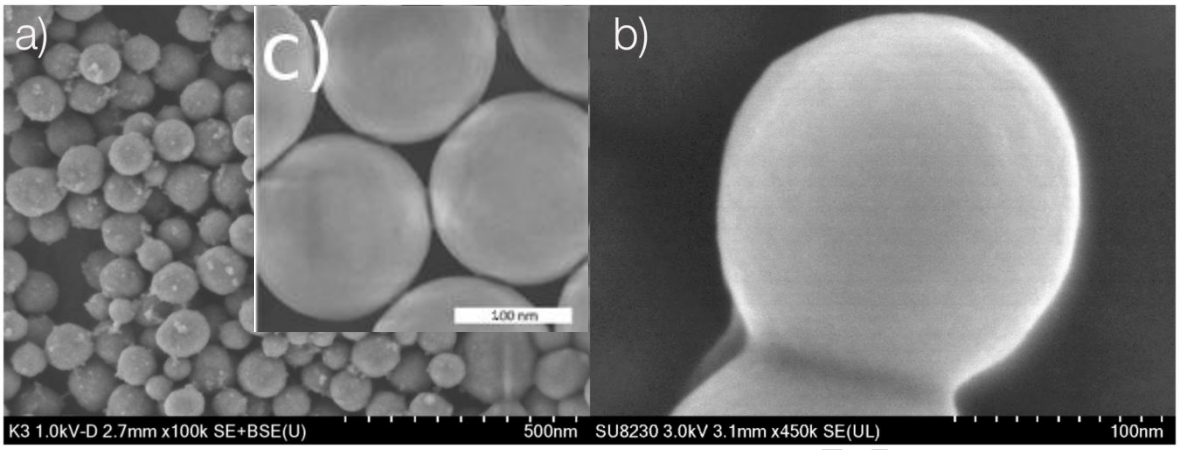

Figure 6. SEM images showing the size, shape and morphology of a) SiNp; b) functional material using G2 compound group; and c) SiNp at the same scale as G2.

Fluorescence spectra of nanomaterials were obtained and adjusted under the same criteria (behavior of *PLi* loss was described by the same one first order exponential decay model) and they can be seen in Figure 7.

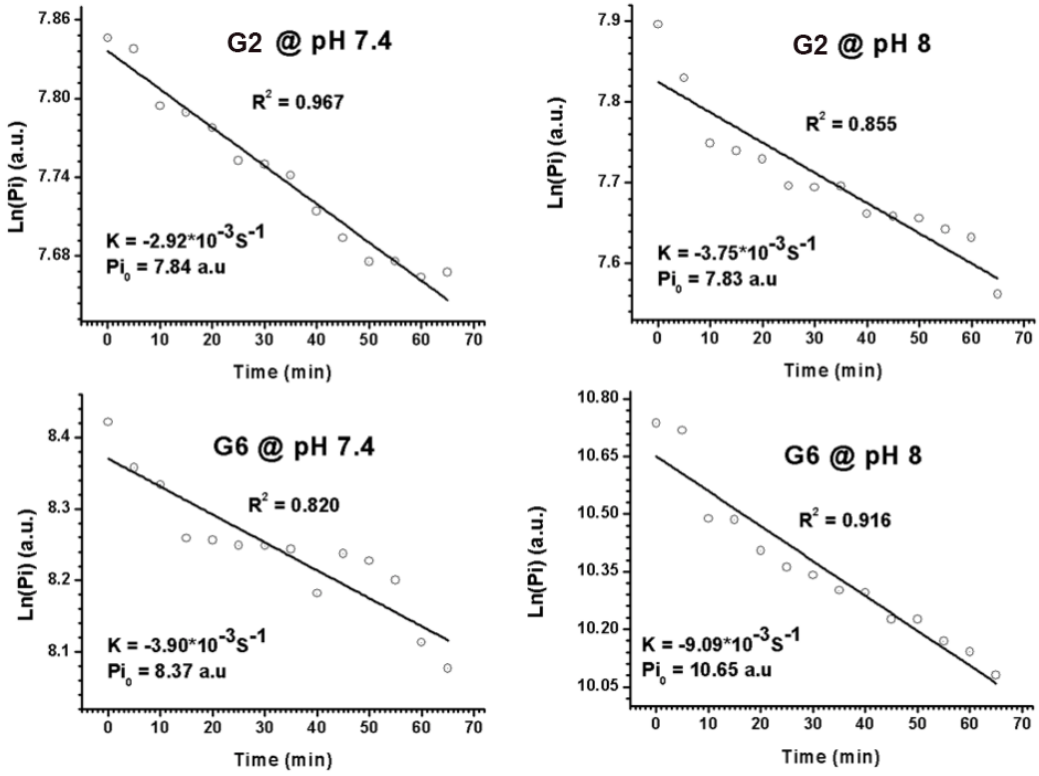

Figure 7. Fluorescence intensity plots at physiological (7.4) an alkaline (8.0) pH media for the nanomaterials obtained from G2 and G6

The exponential decay model fits consistently to experimental data and constant rate *k* describes fluorescence extinction constant of the two nanosystems; SiNp-G2 (N-G2) and SiNp-G6 (N-G6). The lowest proportion of the variance—R^2— was of 0.82 for N-G6 at pH 7.4, while the best fit was found in the nanosystemsN-G2 at pH 7.4 with R^2 of 0.967. The proximity of these values to unity (Figures 5 and 7) is very interesting if one considers that decays of fluorescence intensity in biomolecules often exhibit a complex behavior, the origin of which can result from multiple factors, such as its ground state as conformational dynamics, spectral relaxation, or other interactions between fluorophores and their environment. Normally the fluorescence is described by a multiexponential model, i.e., the arithmetic sum of several exponents characterized by lifetimes and pre-exponential factors basing on the interpretation of each discrete component with the aid of a particular molecular conformation, including dynamic equilibrium between rotational isomers or reversible reactions between reagents/products. The fit with a first order exponential decay model suggests a low complexity decay of fluorescence intensity of these biomolecules, that can attributable to a single chemical specie undergoing a relatively simple and irreversible molecular transformation such as the one suggests by Acuña his report [9].

Table 4. Constants rates and percentage of fluorescence intensity (*PLi*) decay.

		PLi decay [%]	*k* [min^{-1}]	R^2
pH 7.4	G2	10.43	$-1.31*10^{-3}$	0.510
	N-G2	2.29	$-2.92*10^{-3}$	0.967
	G6	27.37	$-3.96*10^{-3}$	0.954
	N-G6	3.68	$-3.90*10^{-3}$	0.820
pH 8.0	G6	16.37	$-1.65*10^{-3}$	0.693
	N-G2	4.18	$-3.75*10^{-3}$	0.855
	G6	24.40	$-3.96*10^{-3}$	0.792
	N-G2	5.96	$-9.09*10^{-3}$	0.916

On the other hand; the fact of having found a value of *k* for each of the five fluorescent groups (Table 3) and the two nanosystems (Table 4), implies that they are different molecules that participates on fluorescence activity; this was already evident from the chromatography sequencing but it was necessary to characterize the fluorescence of each of the groups, to find their physical parameters.

3.3Theoretical calculations of UV-Vis spectra

To understand the underlying mechanism behind the fluorescence, we investigated the electronic properties of the excited states responsible for the emission using quantum chemical calculations. UV-Vis spectra and geometry optimizations of the ground states for G2, G5 and G6 were performed using time dependent density functional theory (TD-DFT) calculations.

The HOMO-LUMO energy gap for G2, G5 and G6 were calculated to be 6.20, 6.27 and 6.35 eV and is in excellent agreement with the experimental UV-Vis absorption, as can be seen in Figure 8 showing good agreement with the experiment and accounting for the finer structure of the bands. Despite the good agreement between experimental (Figure 1) and theoretical UV-Vis plots, some differences can be ascribed to the fact that only the main transition was calculated for the sake of computational simplicity. Table 5 lists the wavelengths to the UV-Vis transitions their oscillator strengths and contributions to the orbital transitions.

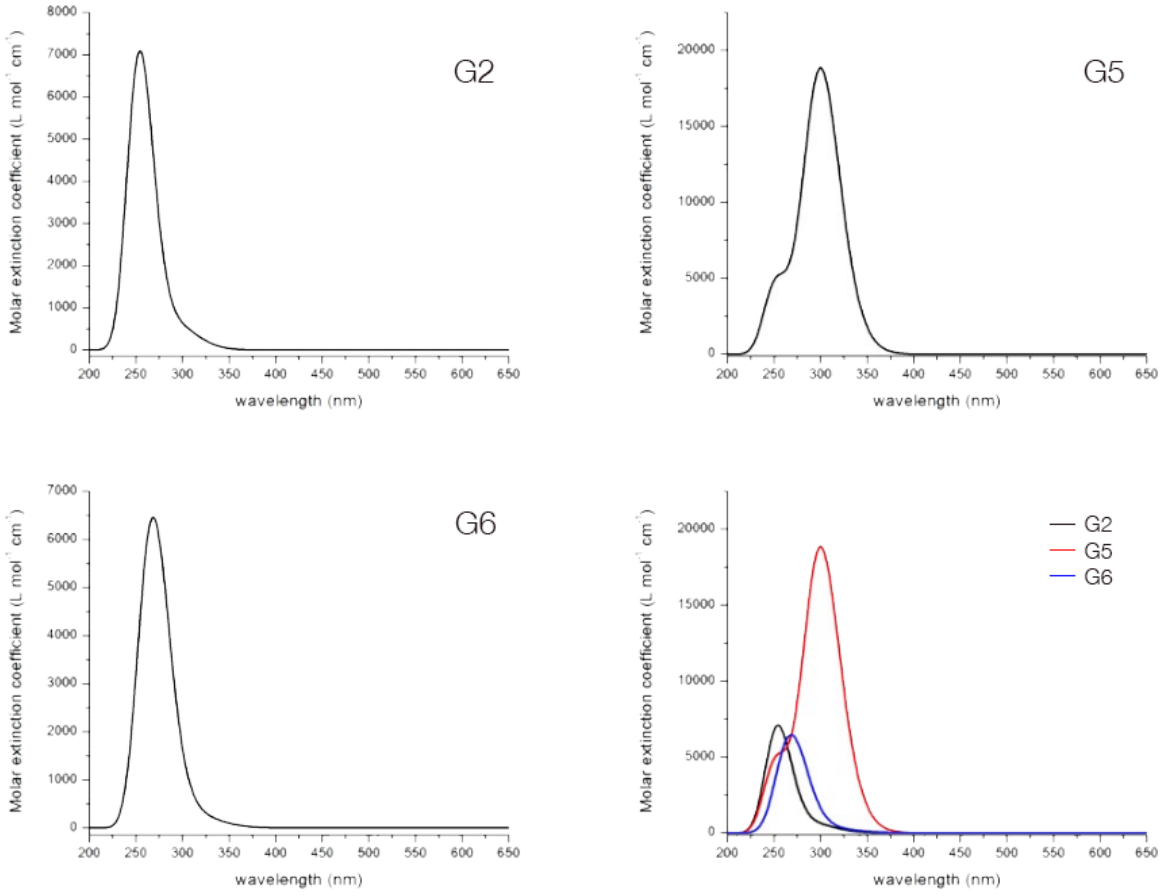

Figure 8. UV-Vis spectra for compounds on G2, G5 and G6 calculated by Density Functional Theory (DFT) from their optimized geometries.

Table 5. Orbital transitions and oscillator strengths to the main electronic transitions for compounds G3,G5 and G6

Molecule Set	Wavelength (nm)	*f*	Orbital Transition	Contribution
G2	255.14	0.1378	HOMO-3 -> LUMO	0.30642
			HOMO-3 -> LUMO+1	0.11778
			HOMO-2 -> LUMO	0.48745
			HOMO-2 -> LUMO+1	-0.19627
			HOMO-2 -> LUMO+2	0.12076
G5	300.21	0.4456	HOMO -> LUMO	-0.24916
			HOMO-2 -> LUMO	0.10852
			HOMO -> LUMO	0.67891
G6	272.80	0.0949	HOMO-5 -> LUMO	-0.17592
			HOMO-3 -> LUMO	-0.17362
			HOMO-2 -> LUMO	0.11497
			HOMO-1 -> LUMO	-0.22960
			HOMO -> LUMO	0.58215

3.4 HMR study

G2 stands out above the other fluorescent compounds due to its stability at pH 7.4, therefore its ^{1}H-NMR spectrum was obtained, which can be seen in the Figure 9. The ^{1}H-NMR spectrum clearly features characteristic bands of two signal patterns; on one hand, typical signals of an isoflavone were observed and on the other signals of a compound that has a very characteristic proton were observed; these peaks coincide with the characteristic ^{1}H-NMR spectrum peaks of the compound product of the oxidation of a chalcone.

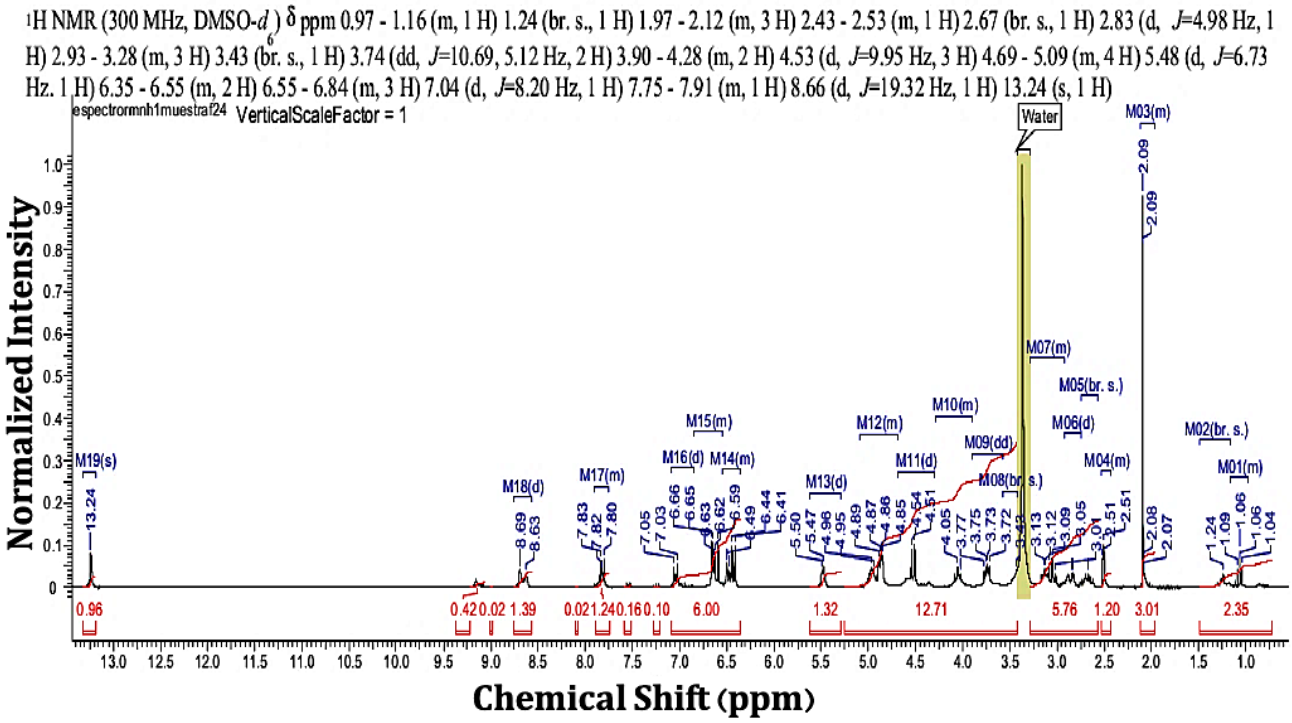

Figure 9. [1]H-NMR spectrum of organic compound/molecule set G2

This result is important since the selected compound group is composed from two different molecules, one isoflavonoids that are referred as molecules with high specificity to estrogens that could be used in an estrogen-depend biological activity[4, 29, 30]and oxidized chalcones (oxacine) that has been reported as fluorescent compounds that could be exploited as biosensor in cells culture since they present this property at physiological pH and also they are reported as non-toxic[9], so its viability in this application is studied onwards.

3.5 Application and viability as biosensor of sample G2

As seen in Figure 10, fibroblast keep their natural morphology without damage appearance in control and treated cells, this is not only seen in the bright field but also the nuclear staining in DAPI panel. In control panel, not specific emission was detected at 488 nm, because the cells are not treated with fluorescence extracts. Even though it is possible to see weak fluorescent signal located in the cellular nucleus, corresponding to the cross emission for DAPI 405 nm. G2 treatment at 488 nm shows homogeneous cytoplasmic localization signal. Nevertheless, with the N-G2 treatment the fluorescence signal appears to be less homogenous observing greater signal with perinuclear localization. This was visualized in Figure 11,

with the 3D reconstruction of the cell where functionalized nanoparticles clustered all around the cellular nucleus. The fluorescent signal at 24 h has a high intensity due to the great stability of the fluorescent compounds when being anchored with the nanoparticle.

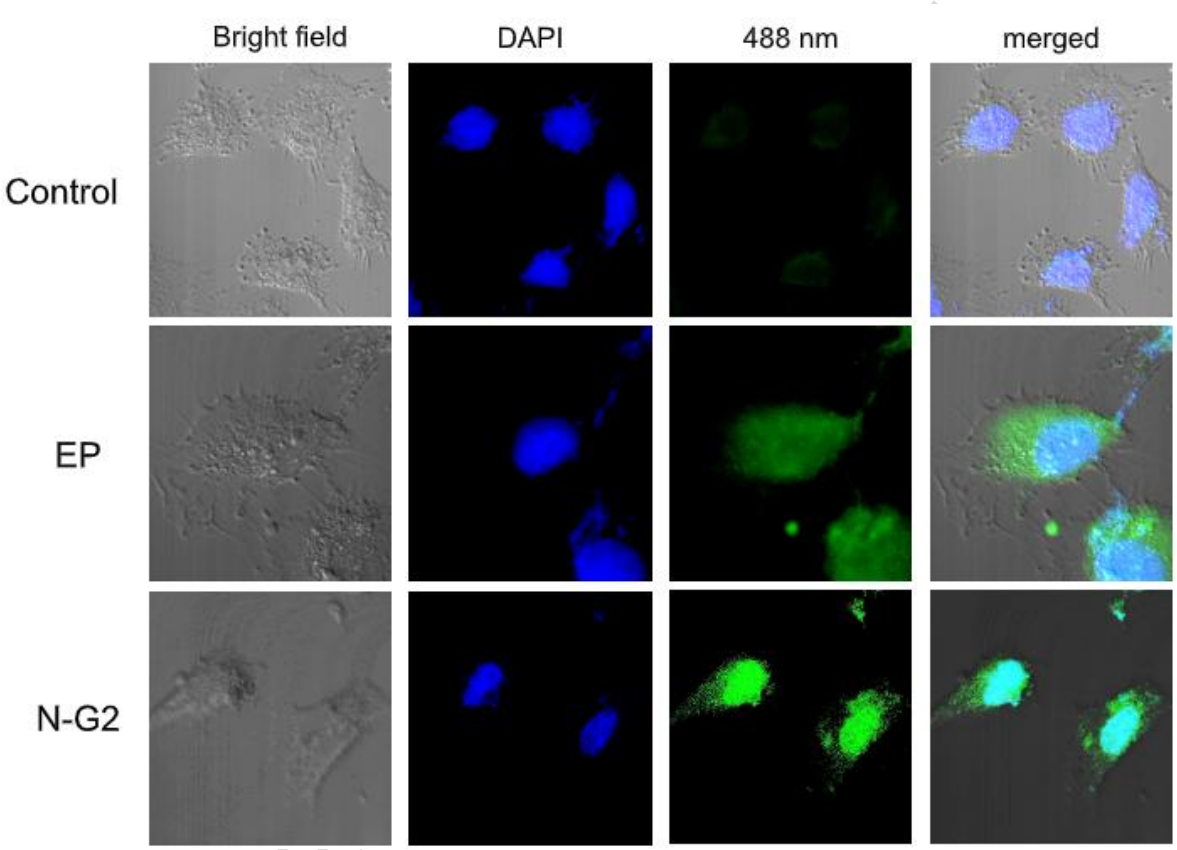

Figure 10. Distribution of selected compound group (G2) and the functional material (N-G2). Cells were incubated for 24 h with 100 ug/mL of G2 compounds group or the functional material from SiNp and selected compounds groups (N-G2) in DMEM medium. Confocal microscopy shows the cells in bright field, nucleus labeling by DAPI at 405 nm, G2 group alone or in N-G2 at 488 nm and image merged.

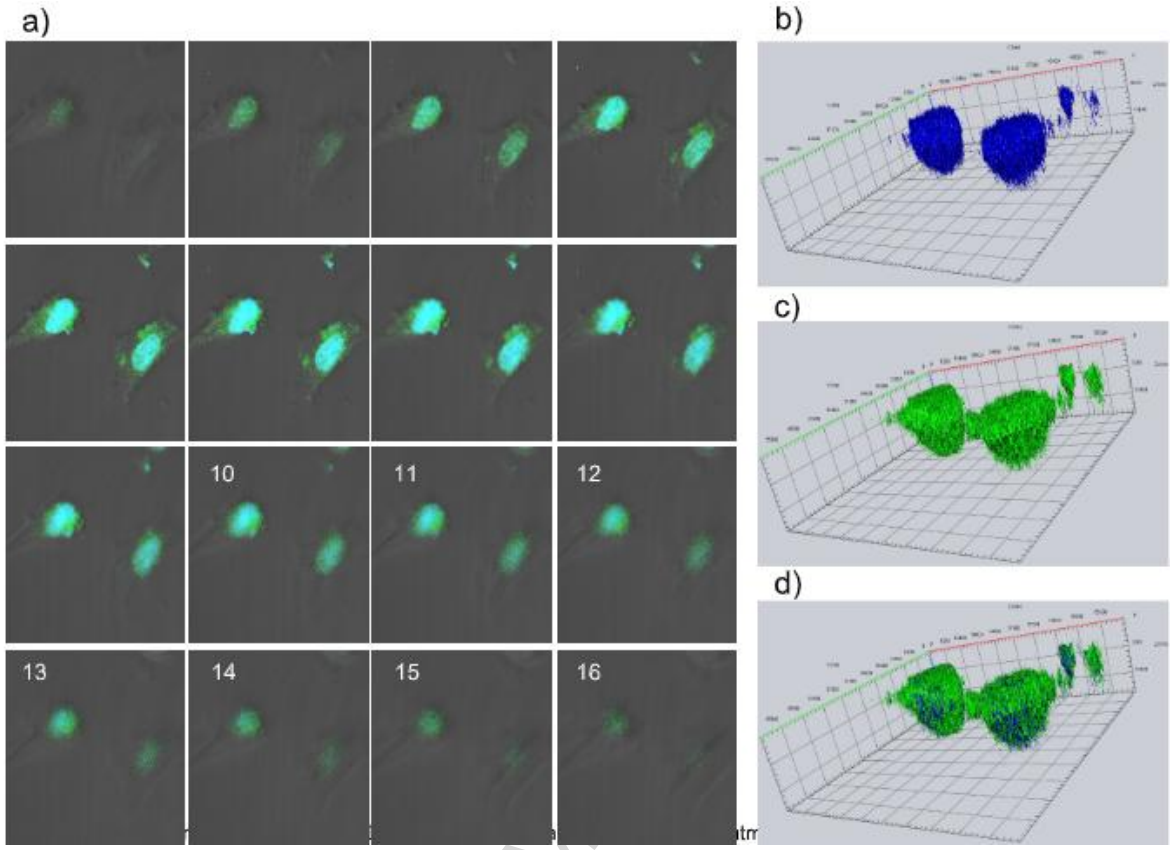

Figure 11. Images stacking for 3D reconstruction of a cell after a 24 h treatment of N-G2 functional material. a) Confocal microscopy images taken in 16 slices (1.12 micron) of a fibroblast cell after treatment with 100 ug/mL of N-G2 for 24 h. DAPI, 488 nm and brightfield channels are shown in merged. The right side of the figure, represents the 3D reconstruction of the cell in panel, b) the nucleus with the DAPI labeling in blue, c) N-G2 presence in green and d) the merged between these two signals where the N-G2 clusters are located all around the nucleus.

Cell viability data were assessed by one-way ANOVA and Tukey significance test with $p < 0.05$. This analysis shows that when normalizing the cell viability of the treatments with respect to their controls, there is no statistically significant difference, between control and treatment (G2 or N-G2) nor between treatments G2 and N-G2. Therefore, this evaluation indicates that there is no apparent cell damage generated by the 24 h treatment of G2 or N-G2 at a dose of 100 µg / mL, so these conditions are not toxic to the cells.

It is important to signalize that the apparent non-toxicity to the cells opens the opportunity for this functional material to be used in biomedical applications, where it could be considering a potential biosensor or nanocarrier due to the cellular internalization, perinuclear localization, and the high fluorescence signal provided by the great stability of *Eysenhardtia polystachia* fluorescent molecules functionalized to SiNp.

These observations lead to further investigation to determine precisely the localization of the N-G2 inside the cell through co-localization of organelle proteins, and other subsequent tests such as the realization of longer courses of time, using different concentrations of treatment in addition to a more in-depth study of cytotoxicity.

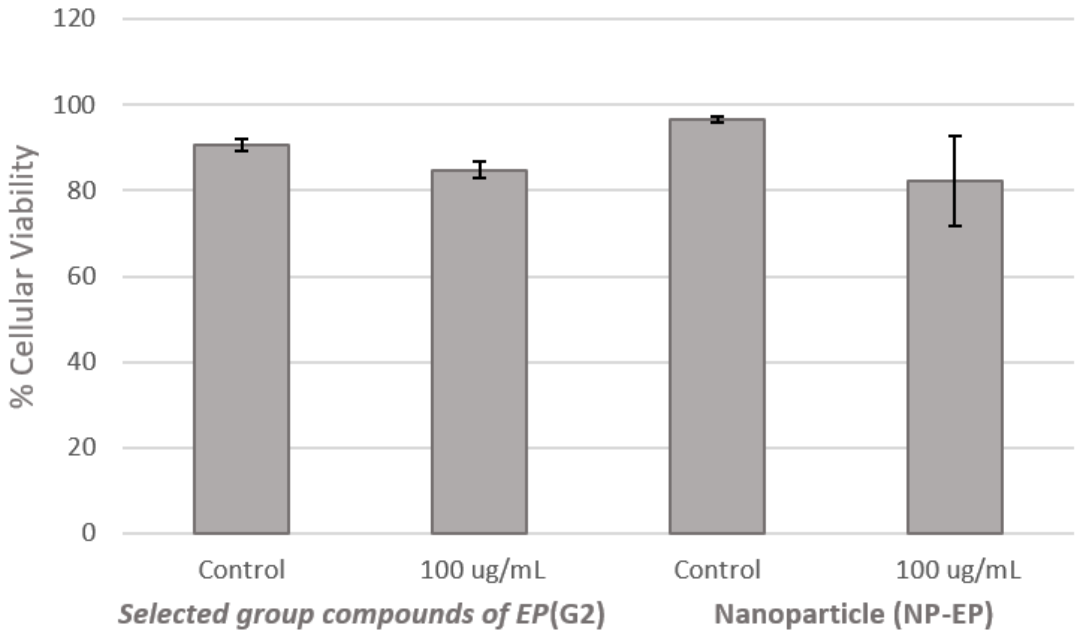

Figure 12. Cellular viability after a 24 h treatment of *Eysenhardtia polystachia* extract (EP) or silica nanoparticles functionalized with the extract of *Eysenhardtia polystachia* (NP-EP). After treatment cellular viability was evaluated by a trypan blue exclusion test and statistical analysis.

4. Conclusions

Previously we explored the viability of using *Eysenhardtia polystachya* in materials with medical applications. Fluorescence and biological activity studies of active principles are essential to determine the proper applications of natural extracts. Other authors reported the main components of EP, but their fluorescence properties had not been studied broadly. Therefore, we studied fluorescent compounds from EP by successfully separating them by column chromatography. Nine fractions were obtained and six of them presented photoluminescence in pH 7.4. Their photoluminescence is shown to be a function of pH, and only four fractions presented photoluminescence in pH 4.0. The more stable (low fluorescence decay) fractions were G2 and G6 that correspond to chalcones and matline chemical species at physiological pH (pH 7.4) from which G2 were tested in order to see their viability as biosensor obtaining promising results because it does not affect cell viability, due to the location of the functional material around the cell nucleus and the clear signal that could have for sensing.

In conclusion, the fluorescence of ethanolic extract of *Eysenhardtia polystachya* depends on more than one chemical specie such as coatline A, B and matline.The four fractions that presented photoluminescence in physiological pH could be used in applications as biosensors, because they are non-toxic and had the proper fluorescent properties.

Acknowledgements

Authors are grateful to MSc. Josefina Barajas for her expertise in the *E. polystachya* sample identification, to Maria Guadalupe Ferreira García and David Fonseca for their support on TLC analysis of samples, to engineers Adrián Hendrik OskamVoorduin, Bernardino Rodríguez-Morales and Gerardo Fonseca for their technical assistance. Also, to Dr. José Antonio Pérez Guzmán for the technical support provided in the digitization and processing of data and images; to A. L. Ramos-Jacques for her valuable contribution in language editing and proofreading of the manuscript. To the "*Laboratorio Nacional de Caracterización de Materiales"* (LaNCaM) for their support on Confocal Lase Microscopy images in cell culture. This research was supported from grants of the "*Dirección General de Asuntos del Personal Académico*" of *"Universidad Nacional Autónoma de México"* through its Program to Support Research Projects and Technology Innovation (UNAM's DGAPA program PAPIIT; Project No. IN209517) and to DGTIC - UNAM for granting access to their supercomputing mainframe 'Miztli'. Finally; One of the authors (A. Rodríguez-Torres) is in debt for the economic support from FOFI-UAQ2018-FNB201802, Universidad Autónoma de Querétaro.

References

[1] L. Alvarez, M.Y. Rios, C. Esquivel, M.I. Chávez, G. Delgado, M.I. Aguilar, M.L. Villarreal, V. Navarro, Cytotoxic Isoflavans from Eysenhardtia p olystachya. Journal of Natural Products, 61 (1998) 767-770.
[2] J.R. Partington, M.B.E., D.Sc. Lignum nephriticum. Annals of Science,11(1) (1955) 1-26.
[3] R. Boyle, Experiments and considerations touching colours. London, (1664), 199-216.
[4] G. Ferreira, A.R. Hernandez-Martinez, H. Pool, G. Molina, M. Cruz-Soto, G. Luna-Barcenas, M. Estevez, Synthesis and functionalization of silica-based nanoparticles with fluorescent biocompounds extracted from Eysenhardtia polystachya for biological applications. Materials Science and Engineering: C, 57 (2015) 49-57.
[5] X.A. Domínguez, R. Franco, Y. Díaz Víveros, Mexican medicinal plants XXXIV. Rotenoids and a fluorescent compound from Eysenhardtia polystachia. Rev. Latinoamer. Quím. 9 (1978) 209-211.
[6] E. Beltrami, M.D. Bernardi, G. Fronza, G. Mellerio, G. Vidari, P. Vita-Finzi, Coatline A and B, two C-glucosil-α-hydroxydihydrochalcones from Eysenhardtia Polystachya. Phytochemistry, 21 (1980) 2931-2933.
[7] L. Alvarez, G. Delgado, C- and O-Glycosyl-α-hydroxydihydrochalcones from Eysenhardtia polystachya. Phytochemistry, 50 (1999) 681-687.
[8] D.T. Burns, B.G. Dalgarno, P.E. Gargan, J. Grimshaw, An isoflavone and a coumestan from Eysenhardtia polystachya-Robert Boyle´s fluorescent acid-base indicator. Phytochemistry, 23 (1984) 167-169.
[9] A.U. Acuña, F. Amat-Guerri, P. Morcillo, M. Liras, B. Rodríguez, Structure and formation of the fluorescent compound of Lignum nephriticum. Organic Letters, 11 (2009) 3020-3023.
[10] Zhong, R., Tang, Q., Wang, S., Zhang, H., Zhang, F., Xiao, M., Man, T., Qu, X., Li, L., Zhang, W., Pei, H., Self- Assembly of Enzyme- Like Nanofibrous G- Molecular Hydrogel for Printed Flexible Electrochemical Sensors. Adv. Mater. 30 (2018) 1706887
[11] X. Qu, D. Zhu, G. Yao, S. Su, J. Chao, H. Liu, X. Zuo, L. Wang, J. Shi, L. Wang, W. Huang, H. Pei, C. Fan, An Exonuclease III- Powered, On- Particle Stochastic DNA Walker. Angew. Chem. Int. Ed. 56, (2017) 1855-1858.
[12] Lin Qi, Mingshu Xiao, Xiwei Wang, Cheng Wang, Lihua Wang, Shiping Song, Xiangmeng Qu, Li Li, Jiye Shi, and Hao Pei; DNA-Encoded Raman-Active Anisotropic Nanoparticles for microRNA Detection. Analytical Chemistry 89 (18), (2017) 9850-9856

[13] Tiantian Man, Wei Ji, Xiaoguo Liu, Chuan Zhang, Li Li, Hao Pei, and Chunhai Fan; Chiral Metamolecules with Active Plasmonic Transition. ACS Nano 13 (4), (2019) 4826-4833
[14] Wei Lai, Lei Ren, Qian Tang, Xiangmeng Qu, Jiang Li, Lihua Wang, Li Li, Chunhai Fan, and Hao Pei. Programming Chemical Reaction Networks Using Intramolecular Conformational Motions of DNA. ACS Nano 2018 12 (7), 7093-7099
[15] Xiangmeng Qu, Shaopeng Wang, Zhilei Ge, Jianbang Wang, Guangbao Yao, Jiang Li, Xiaolei Zuo, Jiye Shi, Shiping Song, Lihua Wang, Li Li, Hao Pei, and Chunhai Fan. Journal of the American Chemical Society 2017 139 (30), 10176-10179
[16] M.G. Ferreira-García, A.R. Hernandez-Martinez, R. Esparza, G.A. Molina, F. Rodriguez-Melgarejo, S. Jiménez, M. Estevez, Effects of extraction solvents on photoluminescent properties of eysenhardtia polystachia and their potential usage as biomarker. Materials Science and Engineering: C, 72 (2017) 42-52.
[17] B.R. Masters, Molecular Fluorescence: Principles and Applications, Second Edition, SPIE, 2013.
[18] M. Muyskens, V. Ed, The Fluorescence of Lignum nephriticum: A Flash Back to the Past and a Simple Demonstration of Natural Substance Fluorescence. Journal of Chemical Education, 83 (2006) 765.
[19] R. Merghem, M. Jay, N. Brun, B. Voirin, Qualitative analysis and HPLC isolation and identification of procyanidins from Vicia faba. Phytochem Anal. 15 (2004) 95-99.
[20] S. Gallori, A.R. Bilia, M.C. Bergonzi, W.L.R. Barbosa, F.F.J.C. Vincieri, Polyphenolic constituents of fruit pulp of Euterpe oleracea Mart. Chromatography 59 (2004) 739-743.
[21] K. Ishiguro, S. Nagata, H. Fukumoto, M. Yamaki, S. Takagi, K. Isoi, A flavanonol rhamnoside from Hypericum japonicum. Phytochemistry, 30 (1991) 3152-3153.
[22] S.L. Greasley, S.J. Page, S. Sirovica, S. Chen, R.A. Martin, A. Riveiro, J.V. Hanna, A.E. Porter, J.R. Jones, Controlling particle size in the Stöber process and incorporation of calcium. Journal of Colloid and Interface Science, 469 (2016) 213-223.
[23] M.E. Echeverri, L.F. Giraldo, B.L. López, Síntesis y funcionalización de nanopartículas de sílica con morfología esférica. Scientia Et Technica, 13(36) (2007) 169-173.
[24] M. Frisch, G. Trucks, H.B. Schlegel, G.E. Scuseria, M.A. Robb, J.R. Cheeseman, G. Scalmani, V. Barone, B. Mennucci, G. Petersson, Inc., Wallingford, CT, 200 (2009).
[25] J.M. Narváez-Mastache, M.L. Garduño-Ramírez, L. Alvarez, G. Delgado, Antihyperglycemic activity and chemical constituents of Eysenhardtia platycarpa. Journal of Natural Products, 69 (2006) 1687-1691.
[26] W. Maciejewicz, M. Daniewski, K. Bal, W.J.C. Markowski, GC–MS identification of the flavonoid aglycones isolated from propolis. Chromatographia, 53 (2001) 343-346.
[27] L.-Z. Lin, X.-G. He, M. Lindenmaier, J. Yang, M. Cleary, S.-X. Qiu, G.A. Cordell, LC-ESI-MS study of the flavonoid glycoside malonates of red clover (Trifoliumpratense). Journal of Agricultural and Food Chemistry, 48 (2000) 354-365.
[28] B. Valeur, Molecular Fluorescence: Principles and Applications. Publisher Wiley (2001) 273-350.
[29] C.S. Hwang, H.S. Kwak, H.J. Lim, S.H. Lee, Y.S. Kang, T.B. Choe, H.G. Hur, K.O. Han, Isoflavone metabolites and their in vitro dual functions: they can act as an estrogenic agonist or antagonist depending on the estrogen concentration. The Journal of Steroid Biochemistry and Molecular Biology, 101 (2006) 246-253.
[30] C. Borrás, J. Gambini, M.C. Gómez-Cabrera, J. Sastre, F.V. Pallardó, G.E. Mann, J. Viña, C., Genistein, a soy isoflavone, up-regulates expression of antioxidant genes: involvement of estrogen receptors, ERK1/2, and NFkappaB. FASEB Journal, 20 (2006) 2136-2138.

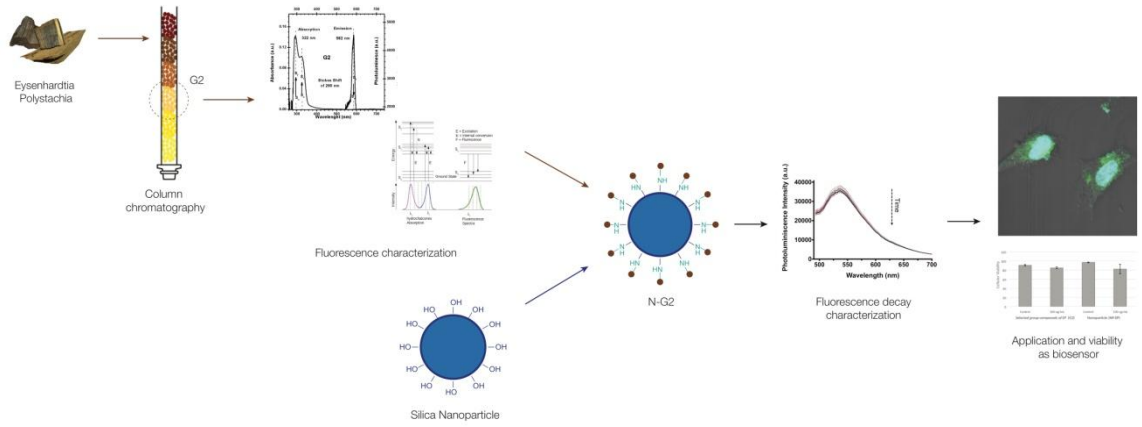

Graphical abstract

Highlights

Eysenhardtia polystachya (EP); an endemic Mexican plant with fluorescence properties

Fluorescent compounds from EP were studied and their fluorescence properties were evaluated.

Fluorescence of ethanolic extracts from EP is due to more than one component

Feasibility of using some components of the "EP" as fluorescent biosensors was demonstrated